Optical integration of SPO mirror modules in the ATHENA telescope

Valsecchi, G., Marioni, F., Bianucci, G., Zocchi, F., Gallieni, D., et al.

G. Valsecchi, F. Marioni, G. Bianucci, F. E. Zocchi, D. Gallieni, G. Parodi, M. Ottolini, M. Collon, M. Civitani, G. Pareschi, D. Spiga, M. Bavdaz, E. Wille, "Optical integration of SPO mirror modules in the ATHENA telescope," Proc. SPIE 10399, Optics for EUV, X-Ray, and Gamma-Ray Astronomy VIII, 103990E (29 August 2017); doi: 10.1117/12.2272997

SPIE.

Event: SPIE Optical Engineering + Applications, 2017, San Diego, California, United States

Optical integration of SPO mirror modules in the ATHENA telescope

G. Valsecchi*[a], F. Marioni[a], G. Bianucci[a], F.E. Zocchi[a], D. Gallieni[b], G. Parodi[c], M. Ottolini[c], M. Collon[d], M. Civitani[e], G. Pareschi[e], D. Spiga[e], M. Bavdaz[f], E. Wille[f]
[a]Media Lario S.r.l., Località Pascolo, 23842 Bosisio Parini, Italy
[b]A.D.S. International S.r.l., via Roma 87, 23868 Valmadrera, Italy
[c]BCV Progetti S.r.l., Via S. Orsola1, 20123 Milano, Italy
[d]Cosine Research B.V, Oosteinde 36, NL-2361 HE Warmond, The Netherlands
[e]INAF Osservatorio Astronomico di Brera, Via E. Bianchi 46, 23807 Merate, Italy
[f]European Space Agency, ESTEC, Keplerlaan 1, NL-2200 AG Noordwijk, The Netherlands

ABSTRACT

ATHENA (Advanced Telescope for High-ENergy Astrophysics) is the next high-energy astrophysical mission selected by the European Space Agency for launch in 2028. The X-ray telescope consists of 1062 silicon pore optics mirror modules with a target angular resolution of 5 arcsec. Each module must be integrated on a 3 m structure with an accuracy of 1.5 arcsec for alignment and assembly. This industrial and scientific team is developing the alignment and integration process of the SPO mirror modules based on ultra-violet imaging at the 12 m focal plane. This technique promises to meet the accuracy requirement while, at the same time, allowing arbitrary integration sequence and mirror module exchangeability. Moreover, it enables monitoring the telescope point spread function during the planned 3-year integration phase.

Keywords: X-ray optics, X-ray telescopes, ATHENA, Silicon Pore Optics, Integration, Optical Alignment,

1. INTRODUCTION

The Advanced Telescope for High-ENergy Astrophysics (ATHENA) is an X-ray space telescope mission [1]–[5] presently in phase A and planned for launch by the European Space Agency (ESA) in 2028. The optics of ATHENA is based on a new technology exploiting the commercial availability of very smooth and thin Silicon wafers and developed by ESA during the last decade. This technology, called silicon pore optics (SPO) [6], [7] allows the realization of stacks of few tens of curved grazing incidence mirrors obtained from the polished side of the wafer and kept separated by thin ribs machined on the back side of the same wafer. The space between ribs are channels ("pores") through which the X-ray radiation enters the optics and is reflected at grazing incidence by the gold-coated polished surface of the wafer. A picture of one SPO stack is shown in Figure 1.

If the wafer mirrors are properly conformed [6], [7], a pair of SPO stacks, one with parabolic-shaped surface followed by one with hyperbolic-shaped surface, can be aligned to realize the Wolter I configuration [8]–[12] often used in X-ray telescopes. In the case of ATHENA, each stack has dimensions ranging between 20.6 mm and 110.0 mm in length and between 49.0 and 101.7 mm in width. The height of the stacks is defined by number of plates, typically 34 for a total of about 28 mm. The set of two pairs of parabolic and hyperbolic stacks, properly aligned and integrated on a support structure called bracket, composes what is called a mirror module (MM).

The current configuration of the ATHENA telescope consists of 1062 of such mirror modules, all with the same focal length of 12 m, tasseled over a physical aperture with a baseline diameter of 3 m. A pictorial representation of the arrangement of the mirror modules is illustrated in Figure 2. Each mirror module needs to be aligned and integrated with adhesive on the overall 3 m supporting structure made of Titanium alloy. The integration process must guarantee a co-alignment of the full set of mirror modules within an uncertainty low enough to limit the degradation of the angular resolution of the final telescope. Since the requirement for the latter is 5 arcsec half energy width (HEW), the error budget allocated for the uncertainty due to alignment and integration of the entire mirror modules population is 1.5

*giuseppe.valsecchi@media-lario.com; phone +39 031 867 111; media-lario.com

Optics for EUV, X-Ray, and Gamma-Ray Astronomy VIII, edited by Stephen L. O'Dell, Giovanni Pareschi, Proc. of SPIE Vol. 10399, 103990E · © 2017 SPIE · CCC code: 0277-786X/17/$18 · doi: 10.1117/12.2272997

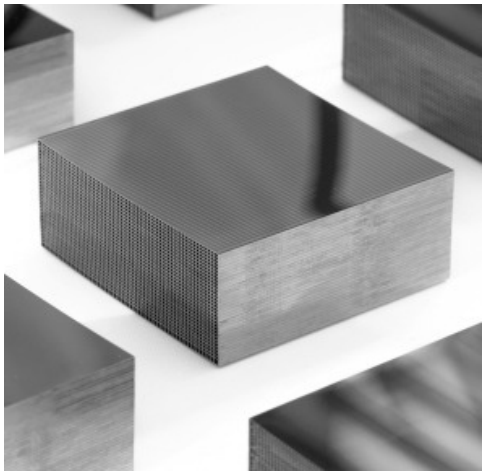

Figure 1. Silicon Pore Optics mirror stack [3].

arcsec, summed in quadrature to other contributions. Moreover, there is a specification on the maximum loss of effective area of the telescope, which is set to 5% for the demonstrator and 1% for the flight model.

One of the proposed approaches for reaching this goal is being tested and validated by this industrial and scientific team under an ESA contract and is based on the ultra-violet imaging at 218 nm of each mirror module on the 12 m focal plane. This approach is based on the extensive heritage left by several X-ray telescopes which the team has worked on, including XMM-Newton [13], eRosita [14], SWIFT [15]. Despite the rather intense diffraction induced by the narrow channels present in each SPO stack (of the order of 1 arcmin in the direction orthogonal to the stack), it has been argued that the position of the centroid of the point spread function (PSF) produced by each mirror module when illuminated by a collimated plane wave is accurate enough to be used as reference for the precise alignment of the mirror module itself. As discussed in the following Section, the concept has been theoretically shown correct [16] and already preliminarily demonstrated experimentally by correlation with X-ray measurement at the PANTER test facility in Munich [18]. After alignment, the mirror modules are fixed to the supporting structure made in Titanium through three dowel pins by means of an adhesive.

From the top technical requirement mentioned above for the integration error budget and the loss of effective area, a set of lower level specifications has been derived for the main functional subsystems, namely the alignment of the mirror modules, the accuracy and stability of the optical bench, and the optical performance of the mirror modules. This set of requirements is listed in Table 1 for both the demonstrator and, preliminarily, the flight module.

The proposed integration approach also satisfies additional requirements, including the request for arbitrarily selecting the integration sequence and the MM exchangeability, independently of the already integrated population. Moreover, the process offers two main advantages since it allows us monitoring: the mirror module PSF during adhesive curing with the possibility to finely tune the alignment in real time; and the telescope PSF during the 3-year integration period. Finally, the proposed method does not need vacuum infrastructure, but only a cleanroom laboratory.

Figure 2. A pictorial view of the 3 m ATHENA optics with the arrangement of the single mirror modules shown.

Table 1. Main and subsystem requirements for the integration of the ATHENA mirror modules for both the demonstrator and, preliminarily, the flight module. X, Y, and Z correspond to azimuthal, radial, and optical axis direction.

Parameter	Demonstrator	Flight Module (Preliminary)
Main Requirements		
HEW	< 1.5 arcsec	< 1.5 arcsec
Effective area loss	< 5%	< 1%
MM alignment		
Max. error in X and Y	< 12 μm	< 12 μm
Max. rotation error in X	< 100 arcsec	< 10 ÷ 30 arcsec
Max. rotation error in Y	< 400 arcsec	< 30 ÷ 120 arcsec
Optical bench		
Collimation of UV beam	> 41 km	> 95 km
Stability of UV beam collimation	> 41 km	> 1500 km
Position accuracy of source in Z	< 160 μm	< 380 μm
Stability of source position in Z	< 160 μm	< 23 μm
Position accuracy of detector in Z	< 3.5 mm	< 1.5 mm
Stability of detector position in Z	< 3.5 mm	< 93 μm
Stability during curing for Z rotation	< 3.2 arcsec	< 1.5 ÷ 9 arcsec
MM optical performance		
Accuracy of MM focal length	< 5 mm	< 1.5 ÷ 2.5 mm
Alignment accuracy of brackets in X and Y	< 0.5 mm	< 0.5 mm

2. MIRROR MODULE METROLOGY AT ULTRAVIOLET WAVELENGTH

The basic concept, on which the proposed alignment and integration approach relies, consists in using optical metrology at ultraviolet light to assess the correct alignment of each mirror module. A plane wave at 218 nm illuminates the mirror module and the position of the centroid of the point spread function on the focal plane is used as figure of merit for the alignment assessment.

The cross section of a SPO mirror module consists of a 2-dimenstional array of square channels or pores with typical dimension of 0.83 mm × 0.83 mm each of which focuses the light to the focal plane after a double reflection on the Wolter I longitudinal profiles. Given the small dimension d of the aperture of each pore with respect to the optical wavelength λ, a strong diffraction of the order of $\lambda/d \approx 54$ arcsec is expected for $d = 0.83$ mm. Actually, the optical path is the same for the pores in each row along the azimuthal direction, whereas it varies from row to row along the radial direction, and the optical path difference is in general much larger than λ. Thus, interference occurs among the rays in each row, whereas the superposition is nearly incoherent among different rows. The resulting diffraction pattern, computed by application of the far-field diffraction theory [17] is shown in Figure 3, where the azimuth corresponds to the horizontal direction on the page. A cross section along this axis is plotted in Figure 4. The good agreement between simulation and the measurement is evident. In particular, the angular separation of 45 arcsec between the diffraction peaks corresponds to the pore period along azimuth of 1 mm [17].

The next point to verify is the correlation between the alignment done using ultra-violet radiation and the corresponding performance at X-ray. To answer this question, numerical and experimental work has been carried out. In the simulations performed in ultra-violet and X-ray light [16] the centroids separation never exceeded 0.2 arcsec, even assuming different kinds of profile imperfections in the SPO plates. Numerically, this provides an upper limit to the error that can be introduced by an optical alignment in ultra-violet light.

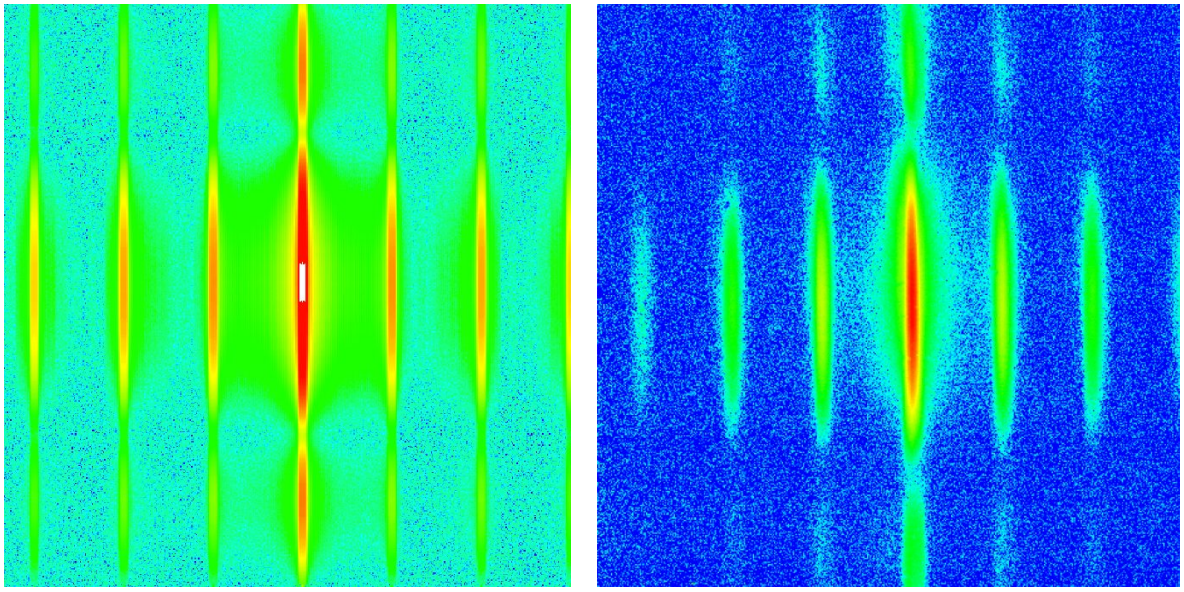

Figure 3. Simulated (left) and measured (right) 2-dimensional diffraction pattern of a mirror module at 218 nm wavelength.

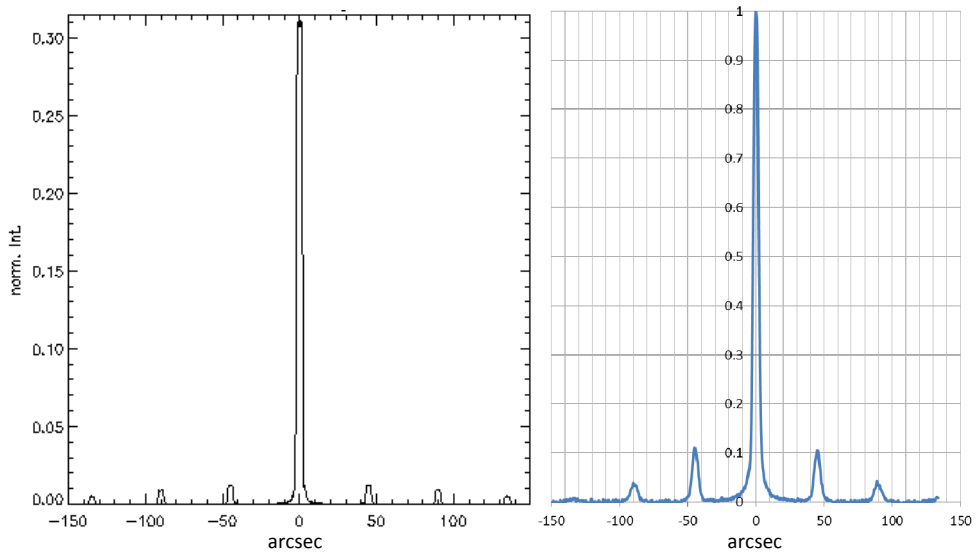

Figure 4. Simulated (left) and measured (right) cross section of the diffraction pattern of Figure 3.

This conclusion was confirmed by the experiment in which mirror module has been measured both at ultra-violet and X-ray and the centroids calculated from the two sets of measurements have been compared. The tests have been performed on a mirror module provided by ESA and Cosine and consisting of one parabolic-hyperbolic pair with 34 plates. Each row of the mirror module has 65 pores with 1 mm pitch, 0.83 mm width, 0.606 mm height. The plates are co-focal and their profile is wedged, hence their incidence angle increases by 2.1 arcsec from one plate to the next.

The mirror module has been measured at ultra-violet light in Media Lario. It was installed on a full-focal length optical bench with its optical axis vertical and illuminated from below by a 218 nm wavelength plane wave. A CCD camera recorded the point spread function on the focal plane. Ten images have been taken, corresponding to ten separate sections of the mirror module along the azimuthal direction, and the corresponding centroids calculated for the main lobe of the diffraction pattern. The results are shown in Figure 5, where the dimension of each point spread function is determined by the light source size of 9 arcsec in diameter along the azimuth (horizontal direction on the page), whereas it is limited by diffraction, with typical angular width of about 54 arcsec, along the radial direction (vertical direction on the page).

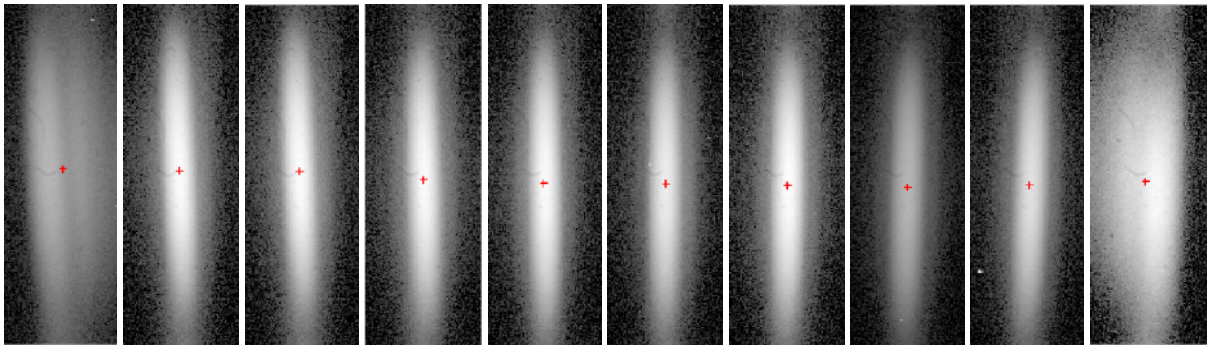

Figure 5. Point spread function and centroid (cross) for ten different azimuthal sections of the mirror module.

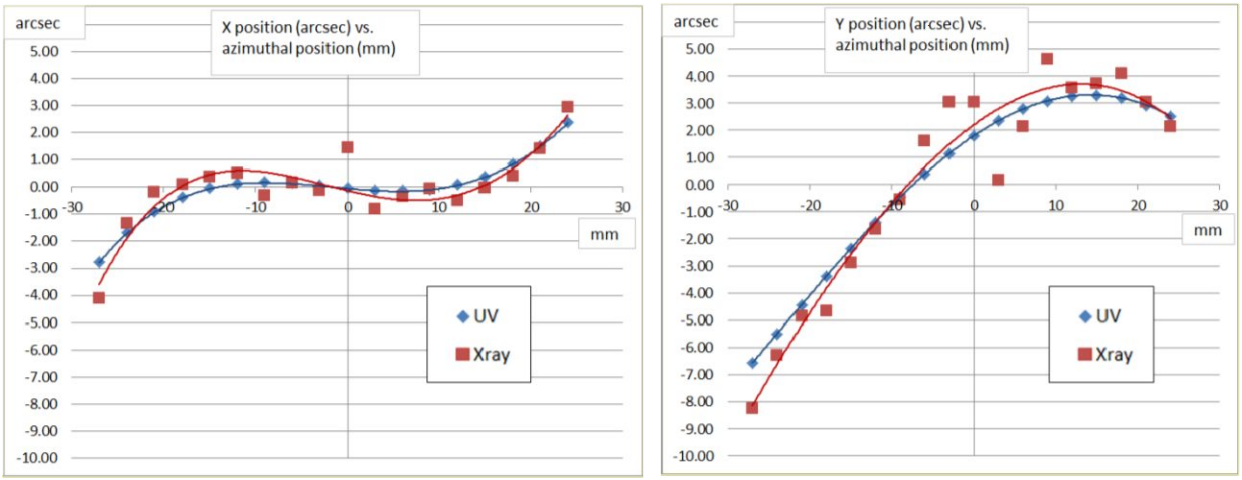

Figure 6. Comparison between the centroid position at ultra-violet and X-ray.

The same mirror module has been also measured at the PANTER test facility in Munich. The mirror module has been scanned with an X-ray beam at 1.49 keV in vacuum, the corresponding point spread function recorded and the centroid position calculated. The correlation between the two sets of measurements have been done by plotting the azimuthal (horizontal) and radial (vertical) shifts of the centroid from the nominal focus as a function of the position of the illuminated area on the mirror module. The result is shown in Figure 6. The standard deviation of the difference between ultra-violet and X-ray centroid position is 0.38 arcsec along azimuth and 0.61 arcsec along the radial direction. In view of the final goal of 0.25 arcsec for this contribution to the overall error budget, the result is very promising since there is ample margin of improvement, which includes:

- at ultra-violet the entire mirror module was measured, whereas at X-ray each pore was illuminated and measured only partially, since the X-ray source was placed at finite distance of 120 m from the mirror module;
- a significant improvement of the ultra-violet optical bench has been implemented and comprises 15 times more powerful and 25 times more stable ultra violet source, more efficient CCD camera, and higher efficiency mirror coating;

the measured mirror module has sectors with half energy width (HEW) between 15 arcsec and 40 arcsec, whereas in perspective the goal of the mirror module HEW is less than 5 arcsec.

3. ATHENA INTEGRATION DEMONSTRATOR

In order to prove the alignment and integration approach proposed for the ATHENA optics, a demonstrator optical bench has been designed and assembled in Media Lario. The structure of the optical bench exploits the facility used for the integration of XMM-Newton [13] X-ray mission but all the instrumentation and optical elements have been completely refurbished as already mentioned in Section 2.

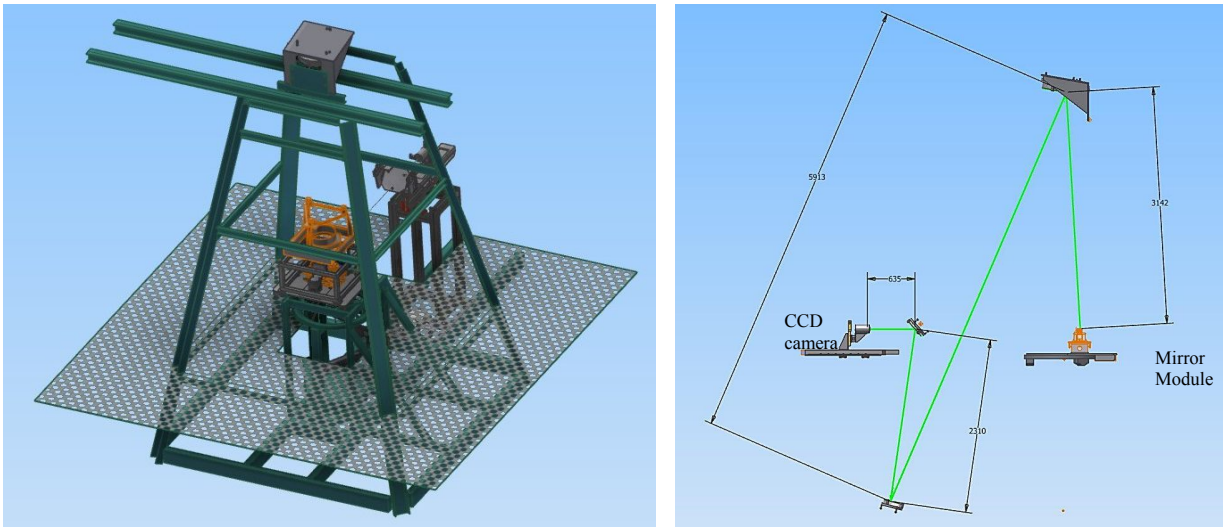

Figure 7. Pictorial representation of the optical bench (left) and sketch of the optical layout from the mirror module to the CCD camera (right). Three flat mirrors are used to fold the 12 m focal length in the available volume.

The optical bench is a collimator where a light source at 218 nm is placed in the focus of a parabolic mirror that produces a plane wavefront and simulates a source at infinite distance. The collimation of this beam has been measured to be better than 45 km. The illuminated mirror module focuses the light into its focal plane at 12 m distance onto a camera that records the point spread function for online processing and calculation of the centroid. A pictorial representation of the optical bench is shown in Figure 7 together with the sketch of the optical path of the ultraviolet light from the mirror module to the camera.

The light source is an uncoherent lamp with a broadband emission spectrum between ultra-violet and infra-red, and provides a diverging beam wide enough to fully illuminate the complete demonstrator. The physical area from which the light is emitted is diaphragmed to a diameter of 50 μm, corresponding to 4.5 arcsec for the 2.3 m focal length parabolic mirror used to generate the plane wave. The power emitted by the source in the bandwidth of 20 nm centered at 218 nm is in the order of few nanowatt.

The detector is a CCD camera with 1024 × 1024 square pixels of 13 μm in side. However, in this application a 2 × 2 pixel binning is used, resulting on an effective pixel size of 26 μm corresponding to 0.45 arcsec over the mirror module focal length on 12 m. The light arriving at the CCD camera is filtered between 208 nm and 228 nm.

In the framework of the project, a mirror structure element (MSE) has been also designed and manufactured to simulate a representative cutout of the final structure on which the 1062 mirror modules will be integrated. The MSE (see Figure 8)

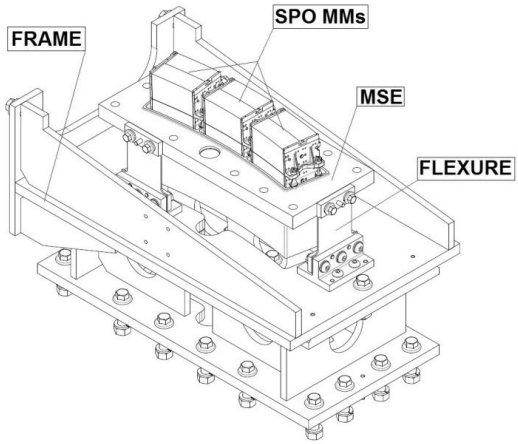

Figure 8. The mirror structure element (MSE) that simulates a cutout of the full mirror structure. The MSE is connected to a frame through 3 flexures that decouple the thermo-mechanical behavior of MSE.

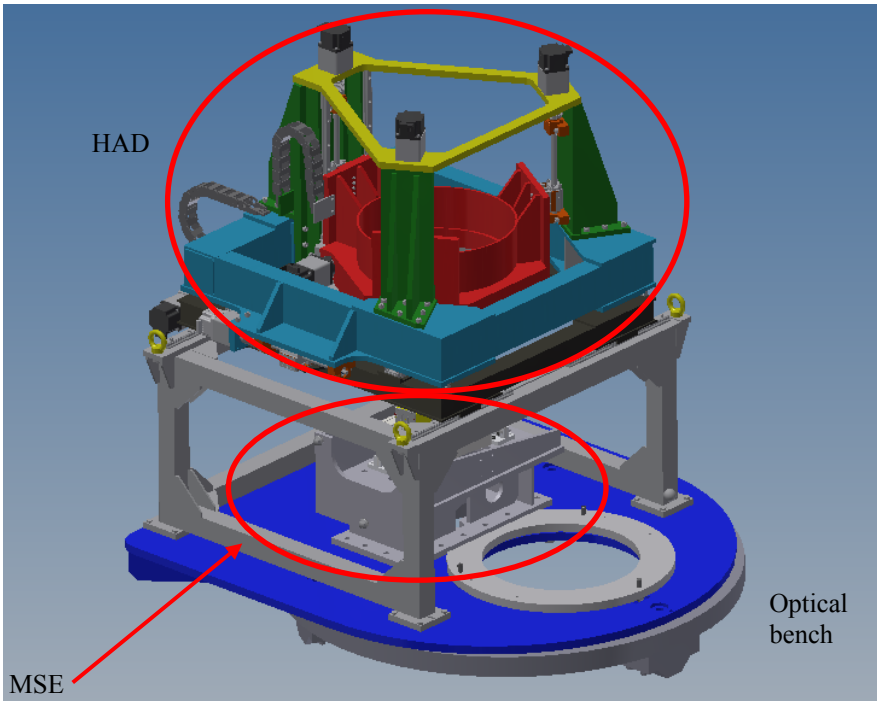

Figure 9. The handling and alignment device (HAD) mounted on the optical bench (cutout) on top of the mirror structure element (MSE).

is made of Titanium and can accommodate 3 mirror modules to allow the full demonstration of the alignment and integration process. The 3 mirror modules are spaced by 7.25° in azimuthal direction and connected to the MSE by three dowel pins each.

The handling and alignment of the mirror module during integration will be performed semi-automatically though a dedicated robotic device. The Handling and Alignment Device (HAD) is the demonstrator machine that has been designed to validate the concept of semi-automatic loading, placement, and fine position adjustment of the mirror modules at their respective locations across the entire X-ray telescope. A pictorial view of the HAD mounted on the optical bench is shown in Figure 9. The required ranges and accuracy of the HAD along the 6 degrees of freedom of the mirror module are listed in Table 2.

The HAD demonstrator is limited in the range of motion in the plane of the telescope (X–Y) plane in order to fly-over the limited region of interest of the MSE. The other features of the machine are fully representative of a full-scale unit and do already allow exploring all the major characteristics of the final device, that include the ability to:

- fine tune the position and attitude of each MM at any orientation angle along the azimuthal coordinate (360° span);
- load, move, and place MMs of different shape, which means different widths and heights;

Table 2. Range and accuracy requirements for the handling and alignment device (HAD).

Degree of Freedom	Range	Accuracy
X translation	±100 mm	±1.3 µm
Y translation	–25 ÷ +90 mm	±1.3 µm
Z translation	120mm	±10 µm
X rotation	± 2°	±20 arcsec
Y rotation	± 2°	±80 arcsec
Z rotation	360°	±3.2 arcsec

- fit its thin positioning arms into the narrow gap existing between the MMs of the different rings;
- natively perform the rotation corrections about two orthogonal MM's axes (X and Y corresponding to azimuthal and radial direction in the telescope frame);
- clamp magnetically the MM by means of permanent magnets.

The X, Y, and Z translations of the HAD are obtained by means of linear stages (2 each for X and Y and 3 for Z) realized with recirculating ball screw driven by stepper motors. Rotations around Z (optical axis of the telescope) are achieved with a fully-steerable rotator (360°) using a custom worm-wheel set coupled to a precision and ultra-thin-section bearing. Rotations around X (azimuth) and Y (radial direction) are more complex to obtain since they need to occur around a virtual pivot in the centre of the mirror module.

Rotation around X is created by a set of flexures properly arranged and shown in Figure 10 (left). The stage holding the MM is pre-loaded by central spring against a stepper linear actuator. The pre-loading force covers about one half of the force budget of the linear actuator. By activating the linear actuator, a rotation about the virtual pivot axis is produced. Rotation around Y (see Figure 10 right) is achieved by means of a swinging platform featuring a couple of guiding arches having a unique axis of rotation. This approach allows creating a stiff axis of rotation projected far beyond the physical mechanical stage.

The refurbishment of the optical bench and the procurement of critical parts is in progress and largely completed. In particular, the structure of the optical bench has been upgraded to match the ATHENA focal length of 12 m. The ultra-violet source and camera are available and a commercial laser tracker for accurate measurement of the focal length (see Section 4) has been procured. Finally, the handling and alignment device is under assembly and testing and will be ready by September 2017. The optical bench qualification and verification of the integration procedures of the mirror module of ATHENA is planned by the end of the year 2017.

4. OUTLINE OF THE ATHENA FLIGHT MODULE INTEGRATION

Along with the design, procurement, and test of the demonstrator integration facility, a preliminary analysis of the flight module integration equipment has been performed. The main constraints and requirements posed by the integration of the full ATHENA optics consists in generating the reference ultra-violet plane wave spatially correlated over the full 3 m aperture of the telescope; in achieving and maintaining the required level of collimation as indicated in Table 1; and in keeping the integration rate of two mirror modules per day.

The proposed solution for generating the collimated ultra-violet beam used as reference for the integration of the mirror modules is to implement a dedicated optical bench equipped with a large 3 m monolithic parabolic mirror, which cover

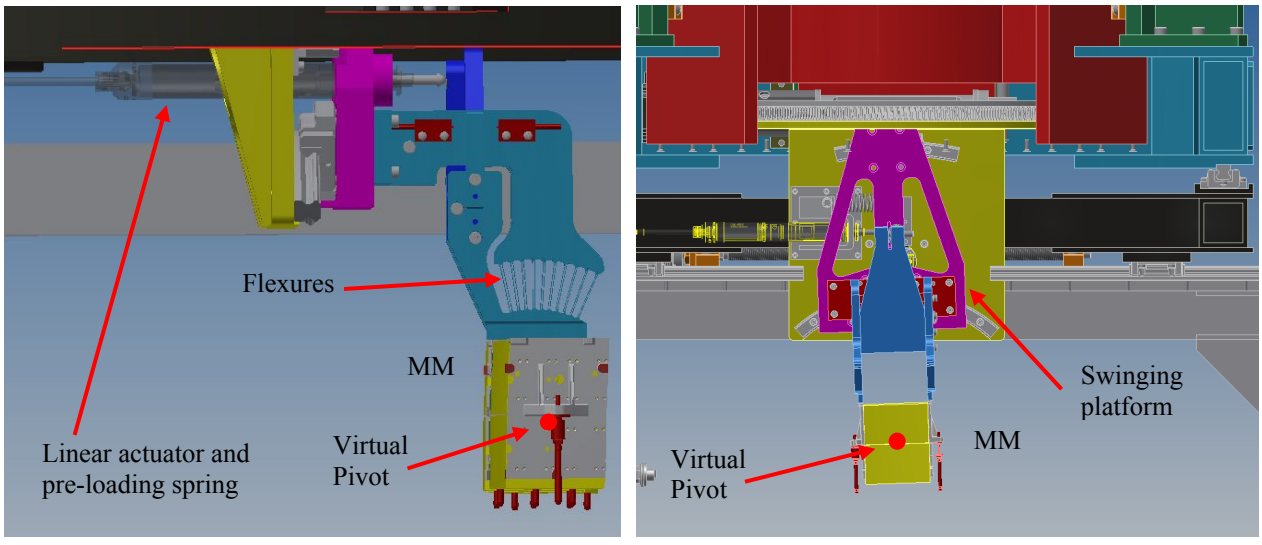

Figure 10. Rotation mechanism around X (left) and Y (right) of the handling and alignment device (HAD). The axis of rotation is normal to the page in both cases.

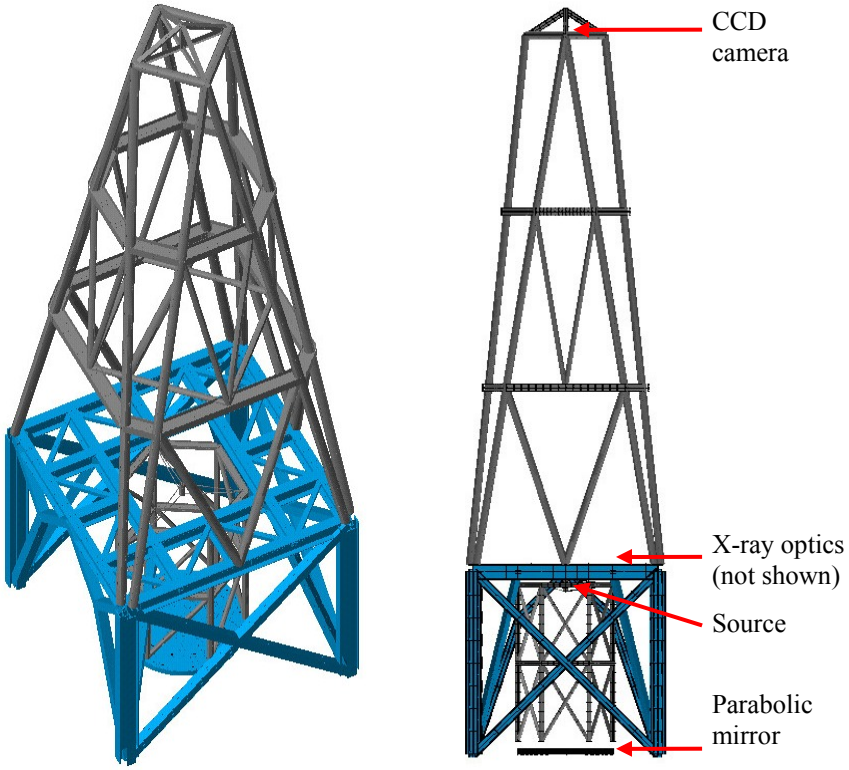

Figure 11. Sketch of a possible configuration of the optical bench for the integration of the Athena flight module. Isometric view (left) and front view (right).

the entire aperture of the X-ray telescope. With respect to other solutions, for example based on smaller parabolic mirror that can be moved where needed across the aperture, the suggested approach appears more reliable since avoid the need of precise and controlled displacement and the related stability issues. A conceptual sketch of a possible configuration of the optical bench is shown in Figure 11.

The accuracy and, particularly, the stability of the collimation of the plane wave produced by the parabolic mirror is very stringent, as indicated in Table 1. Assuming a focal length of 6 m, this corresponds to a stability in the displacement of the source from the focus of the parabolic mirror by 23 μm along the optical axis. Similarly, the stability of the CCD detector should be better than 93 μm (see again Table 1). In order to get accurate measurement of distances a commercial laser tracker has been procured with an accuracy of about 0.01 mm.

Finally, the integration rate of the mirror modules in the X-ray telescope of the ATHENA flight module is essentially limited by the alignment, metrology, and bonding of the mirror module into the mirror structure (about 4 h) and by the curing time of the adhesive ranging between 4 h and 16 h depending on the selected material. This implies that the full integration can take place in a time interval between about 8 h and 20 h. Given the requirement of integrating two mirror modules per day, it may be necessary to install two HADs on the optical bench, particularly in case an adhesive with long curing time is selected.

5. CONCLUSIONS

Preliminary analysis and experimental verification have provided very promising indications that the centroid of the point spread function of each ATHENA mirror module under ultra-violet illumination can be used as an effective figure of merit for the assessment of the alignment of the mirror modules. Moreover, comparison with actinic measurements performed at the PANTER test facility have also shown the excellent correlation between the optical alignment at ultra-violet wavelength and the performance at X-ray.

The optical bench for the demonstration and validation of the proposed approach for the alignment and integration of the

1062 mirror modules of the ATHENA X-ray telescope is at an advanced stage of implementation and will be completed by the end of the summer 2017. By the end of year, the optical bench will be calibrated and tested, and three mirror modules will be integrated onto the mirror structure element. The resulting optics will then be measured at X-ray at the PANTER facility for the final validation of the proposed integration method.

ACKNOWLEDGMENTS

The authors gratefully thank all the members of the team contributing to the project. We also thank the PANTER test facility at the Max Planck Institute for Extraterrestrial Physics for the actinic measurements of the ATHENA mirror module. The work has been done in the framework of the European Space Agency contract 4000114931/15/NL/HB.

REFERENCES

[1] ESA, ATHENA: Assessment of an X-Ray telescope for ESA Cosmic Vision Program, CDF-150(A) (2014).
[2] <http://www.the-athena-x-ray-observatory.eu>.
[3] <http://sci.esa.int/cosmic-vision/54517-athena>.
[4] Ayre, M., Bavdaz, M., Ferreira, I., Wille, E., Fransen, S., Stefanescu, A., Linder, M., "ATHENA – System studies and optics accommodation," Proc. SPIE 9905, 990526 (2016).
[5] Willingale, R., Pareschi, G., Christensen, F., den Herder, J.W., "An Athena+ supporting paper: The Optical Design of the Athena+ Mirror," <http://www.the-athena-x-ray-observatory.eu/images/AthenaPapers/SP14_mirror.pdf>.
[6] Collon, M.J., Ackermann, M., Günther, R., Chatbi, A., Vacanti, G., et al. "Making the ATHENA optics using Silicon Pore Optics," Proc. SPIE 9144, (2014).
[7] Collon, M.J., Vacanti, G., Günther, R., Yanson, A., Barrière, N., et al., "Silicon pore optics development for ATHENA," Proc. SPIE 9603, (2015).
[8] Wolter, H., "Mirror systems with glancing incidence as image-producing optics for X-rays," Ann. Phys. 10, 94–114 (1952).
[9] Chase, R. C. and Van Speybroeck, L. P., "Wolter-Schwarzshild telescopes for X-ray astronomy," Appl. Opt. 12, 1042–1044 (1973).
[10] Giacconi, R., Reidy, W.P., Vaiana, G.S., VanSpeybroeck, L.P. and Zehnpfennig, T., "Grazing incidence telescopes for X-ray astronomy," Space Sci. Rev., 9, 3–57 (1969).
[11] Turner, M.J.L., Flanagan, K.A. (editors), Space Telescopes and Instrumentation 2008: Ultraviolet to Gamma Ray, Proc. SPIE 7011, (2008).
[12] Hoover, R.B., Walker, B.C. (editors), X-ray/EUV optics for astronomy, microscopy, polarimetry, and projection lithography, Proc. SPIE 1343, (1991).
[13] Gondoin, Ph., de Chambure, D., Van Katwijk, K. , Kletzine, Ph. , Stramaccioni, D., Aschenbach, A., Citterio, O., Willingale, R., "The XMM Telescope," Proc. SPIE 2279, 86–100 (1994).
[14] Burwitz, V., Predehl, P. , Friedrich, P. , Bräuninger, H., Eder, J., et. al., "The calibration and testing of eROSITA X-ray mission assemblies," Proc. SPIE 9144, (2014).
[15] Burrows, D.N. , Hill, J.E., Nousek, J.A., Wells, A.E., Short, A.T., Willingale, R., et. al., "Swift X-ray telescope," Proc. SPIE 4140, (2000).
[16] Spiga, D., Della Monica Ferreira, D., Shortt, B., Bavdaz, M., Bianucci, G., Civitani, M., Christensen, F., Collon, M., Conconi, P., Fransen, S., Marioni, F., Massahi, S., Pareschi, G., Salmaso, B., Tayabaly, K., Valsecchi, G., Westergaard, N., Wille, E., "Optical simulations for design, alignment, and performance prediction of silicon pore optics for the ATHENA X-ray telescope," Proc. SPIE 10399, this conference.
[17] Spiga, D., Christensen, F., Bavdaz, M., Civitani, M., Conconi, P., Della Monica Ferreira, D., Knudsen, E., Massahi, S., Pareschi, G., Salmaso, B., Shortt, B., Tayabaly, K., Westergaard, N., Wille, E., "Simulation and modeling of silicon pore optics for the ATHENA X-ray telescope," Proc. SPIE 9905, 99055O (2016).
[18] <http://www.mpe.mpg.de/heg/panter>.